journal

J. Am. Ceram. Soc., 87 [8] 1571–1574 (2004)

Sintering Behavior and Properties of Iron-Rich Glass-Ceramics

Alexander Karamanov,† Giuliana Taglieri, and Mario Pelino*

Department of Chemistry, Chemical Engineering and Materials, University of L'Aquila, 67040 Monteluco di Roio, L'Aquila, Italy

Iron-rich glass-ceramics were obtained by the sintering of two glass powders, labeled G1 and G2, at heating rates of 5° and 20°C/min followed by an isothermal step in the 850°–1050°C temperature interval. The sintering process was evaluated by the linear shrinkage; the closed porosity was estimated by density measurements; the structure and the morphology of the glass ceramics were observed by scanning electron microscopy. The bending strength, the Young modulus, and Vickers hardness of the glass-ceramics materials were evaluated. The results showed that the sintering process and morphology of the glass-ceramics depends on the amount of magnetite and pyroxene formed. With a low percentage of crystal phase formed (25%–30% typical of G1) the structure is characterized by closed porosity; at higher crystallization (45%–50% typical of G2) open porosity is mainly formed. The properties of the glass-ceramics were not influenced by the heating rate but improved with an increase in the degree of crystallization.

I. Introduction

SILICATE compositions containing 10–15 wt% iron oxides are mainly used by the fused-rock industry, which is based on melting natural basalt rocks.[1–3] The products are characterized by high chemical durability and resistance to abrasion and corrosion. Basalt-like compositions were also developed for nuclear waste disposal[4,5] and for the stabilization of iron-rich hazardous industrial wastes, such as jarosite and goethite, arising from the hydrometallurgy of zinc ores[6–8] and electric arc furnace dusts.[9–11]

The high iron content compositions are characterized by a high liquid immiscibility,[6,7] often leading to spontaneous magnetite crystallization. The formation of different liquid and crystal phases increases the apparent viscosity of the melt[12,13] and causes difficulties in forming and shaping. For this reason, iron-rich glass and glass-ceramics are mainly produced by casting, fast-pressing, or centrifuging of the melt.[1] The sintering technique may also be used to improve appearance[14] and properties[15] and to obtain materials with more complicated shapes.[16]

During the production of the sintered glass-ceramics, the formation of the crystalline phases may influence the sintering process. In the sintered glass-ceramics with cordierite[17] or anorthite[18] compositions, the sintering reaches 85%–90% of the theoretical density before the beginning of the crystallization; the degree of densification does not improve by increasing the temperature due to the formation of high percentages of crystal phases. To improve the densification, parent glasses with lower crystallization rate are usually used.[19,20]

The iron-rich glasses form lower percentages of crystal phase than common glass-ceramics (maximum 55%–65%),[6,7] but the crystallization rate is very high. As a result the sintering process occurs at temperatures higher than the crystallization interval.[15]

In the present work, the results of sintering in air of two iron-rich glass powders are presented and discussed. The sintering process was investigated by measuring the linear shrinkage and closed porosity and by observing the structure of the fracture by scanning electron microscopy (SEM). The mechanical properties of the sintered materials were measured and discussed.

The sintering behavior of the same glass compositions, in N_2 inert atmosphere, will be presented and discussed in a second paper.

II. Experimental Procedure

The parent glasses were prepared by mixing jarosite, a waste from hydrometallurgy of zinc, granite waste, sand, and Na_2CO_3. The melting was conducted in a pilot-scale melting kiln, producing granulated glass frit.[8] The furnace is lined with electrofused ZrO_2–Al_2O_3–SiO_2 refractory, and the heating is obtained by liquid petroleum gas (LPG) combustion. The unit can operate continuously with a capacity of 1000–1200 kg/(24 h) or discontinuously at 250–300 kg/batch. In the present set of experiments, about 200 kg of glass frit from each composition was quenched after 5–6 h of melting at 1400°–1420°C. Table I reports the chemical compositions of the glasses used in the present work, measured by a Spectro-Xepos X-ray fluorescence apparatus. A portion of the glass frits was milled and sieved.

The crystallization process was evaluated in non-isothermal conditions by means of thermogravimetric–differential thermal analysis (TG-DTA) ("Netzsch STA 409" apparatus) using about 100 mg of powder sample (45–75-μm particle size) at 5°, 10°, and 20°C/min heating rate in air. The crystalline phases formed were determined by XRD technique (Philips PW1830 apparatus and Cu*K*α radiation). The crystalline fraction was estimated by comparing the areas of the amorphous halo in the spectra of the parent glass and glass-ceramics, respectively. The ratio between the crystalline phases was evaluated by comparing the intensities of the major peaks.

Green samples with dimensions 50/4/4 mm^3 were prepared by mixing the glass powder (45–75-μm fraction) with a 7% poly(vinyl alcohol) (PVA) solution and by pressing at 100 MPa.

Table I. Chemical Compositions of the Investigated Glass Compositions G1 and G2

	SiO_2	Al_2O_3	Fe_2O_3†	CaO	ZaO	PbO	K_2O	Na_2O	Other
G1	47.7	5.6	18.9	6.8	4.6	0.5	2.2	10.3	2.1
G2	42.9	5.8	25.2	9.6	5.6	0.7	2.1	6.5	1.1

†Iron oxides are presented as Fe_2O_3.

G. W. Scherer—contributing editor

Manuscript No. 186812. Received July 26, 2002; approved March 27, 2004.
*Member, American Ceramic Society.
†Author to whom correspondence should be addressed. e-mail: karama@ing.univaq.it.
‡Figures 2 and 3, three views of Figures 8 and 9, and Table II are available on the Internet at www.ceramicjournal.org/datadepository or by fax, 614-794-5822. See or request Data Depository File No. ACD-400.

After drying and a preliminary 30-min step at 280°C (to eliminate the PVA), the samples were treated in air at heating rates of 5° and 20°C/min, held at different temperatures in the 800°–1150°C range for times between 1 and 180 min and cooled at 10°C/min. The sintering was evaluated by measuring the linear shrinkage related to the initial size of 50 mm.

The *apparent* densities of the sintered samples were measured by He displacement pycnometer (AccyPyc 1330).[21] Then, to obtain the *ultimate* density, the samples were crushed and milled to a size below 45 μm, and the density was measured again.[21] Density measurements, conducted on the finer fraction, below 38 μm, did not significantly change the ultimate density value.

The morphology of the samples was examined by SEM (Philips XL30CP).

Glass samples were heated at 5° and 20°C/min and sintered for 1 h at 970°C for G1 and at 1050°C for G2. The mechanical properties were measured after sintering. The bending strength was determined by a three-point bending test with 40-mm outer span and a speed of 0.1 mm/min (SINTEC D/10). The Young modulus was determined by means of the nondestructive resonance frequency technique (Grindosonic). The Vickers hardness was estimated by WOLPERT apparatus.

III. Results and Discussion

(1) Sintering and Crystallization

In Fig. 1 the TG-DTA traces, at 10°C/min heating rate, of G1 and G2 glasses are plotted. They present the typical behavior of iron-rich powder glasses heat-treated in air.[6,7,11] The TG traces (dashed lines) show a detectable increase in weight of 0.5 ± 0.05% for G1 glass and 0.6 ± 0.05% for G2, taking place in the 550°–800°C range. Wide exothermal effects in the DTA trace (solid line) are connected to the weight gain with the maximum at 730° and 660°C for G1 and G2, respectively. As discussed in detail in previous works,[6,7,14] the Fe^{3+}/Fe^{2+} ratio for similar compositions ranges between 6 and 8 and the exotherm and weight gain are due to the oxidations of FeO to yield Fe_2O_3. The crystallization exo-peaks occur at 833° and 852°C, respectively, while the melting of the crystal phases is indicated by the endotherms at 1070° and 1100°C for G1 and at 1150° and 1210°C for G2, respectively.

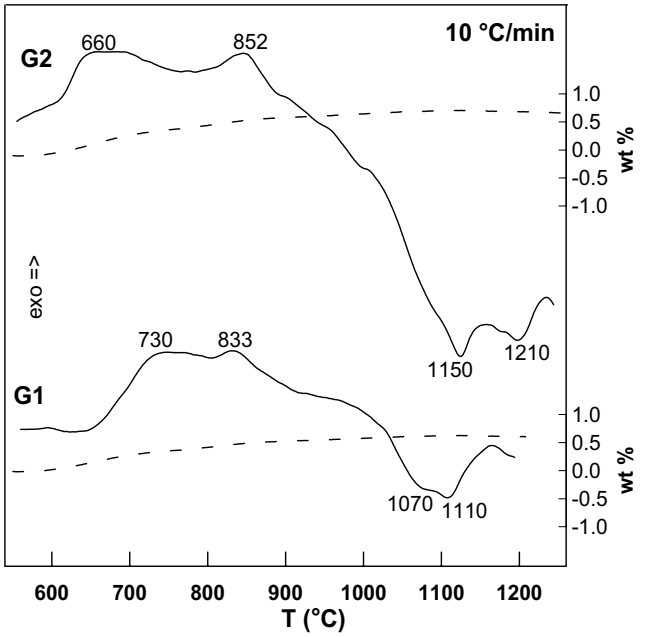

Fig. 1. DTA traces of the parent glass powders G1 and G2 in the range 550°–1250°C.

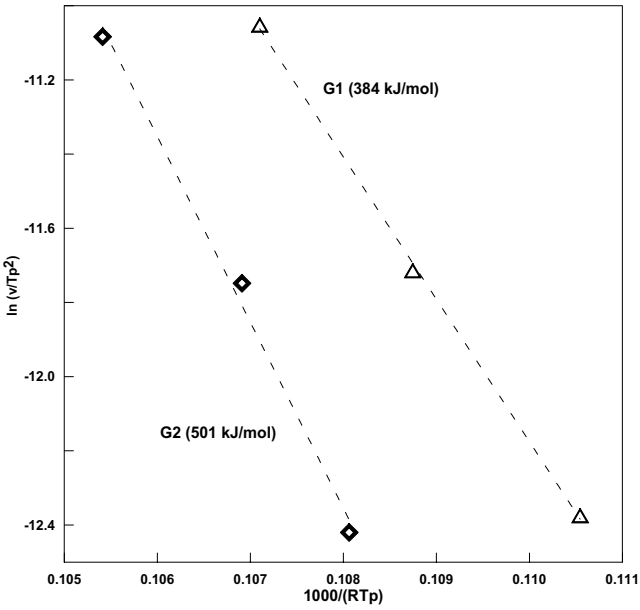

Fig. 4. Kissinger plots and the activation energy of crystallization, E_C, of G1 and G2.

To evaluate the activation energy of crystallization, E_C, additional DTA experiments were conducted at 5° and 20°C/min, up to 1000°C. The E_C was estimated by the Kissinger equation:[22]

$$\ln (v/T_p^2) = -E_C/RT_p + \text{constant} \quad (1)$$

where T_p is the peak temperature of and v is the heating rate. A plot of $\ln (v/T_p^2)$ vs $1/RT_p$ is a line, whose slope corresponds to E_C.

The DTA results are reported in Fig. 2 and Fig. 3 (which are given in the Data Depository (see footnote ‡ on p. 1)), while Fig. 4 shows the Kissinger plots and the corresponding E_C values, which are comparable with similar glass compositions.[14]

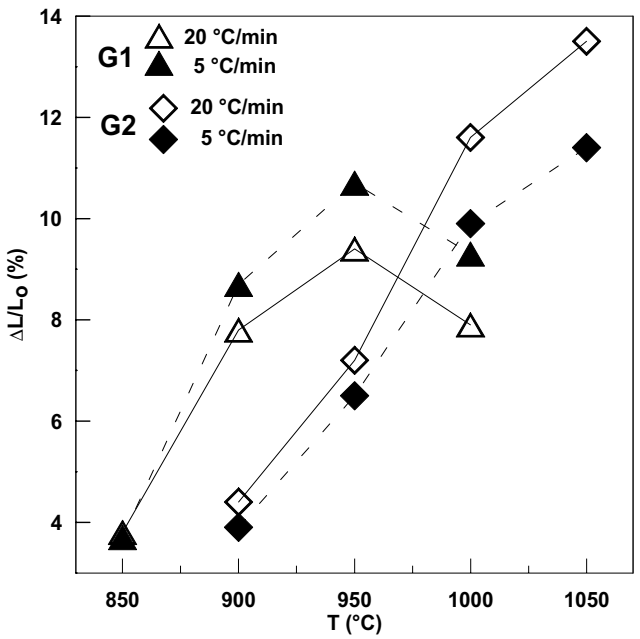

Fig. 5. Linear shrinkage as a function of a 1-h step of the holding temperature.

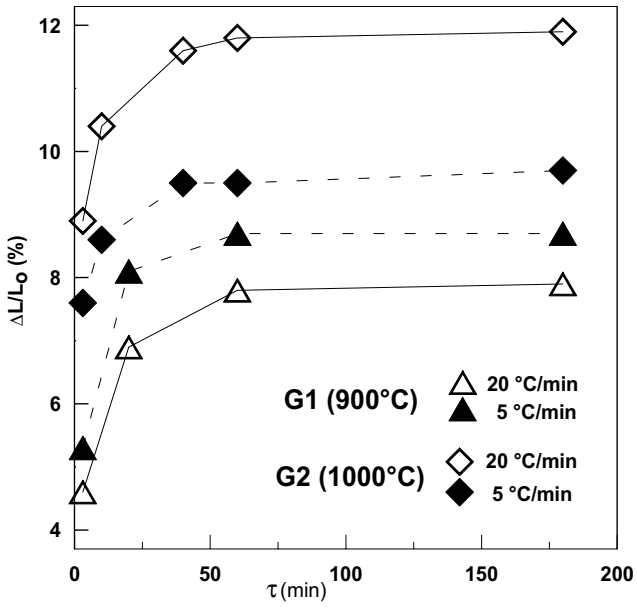

Fig. 6. Linear shrinkage as a function of the holding time at 900°C for G1 and 1000°C for G2.

The XRD analysis highlighted the amorphous structure of the parent glasses and the formation of magnetite (Fe_3O_4) and pyroxene solid solutions ($MgO_x{\cdot}FeO_{1-x}{\cdot}CaO{\cdot}2SiO_2$) in the glass-ceramics. The spectra of the glass-ceramics, sintered at 5°C/min heating rate followed by a 1-h step at 970°C for G1 and at 1050°C for G2 showed the formation of 6.0 ± 3.0 wt% magnetite and 22.0 ± 3.0% pyroxene in G1 and 13.0 ± 3.0 wt% magnetite and 35.0 ± 3.0% pyroxene in G2, respectively. The higher amount of crystal phase formed in G2 glass-ceramic can be related to the higher percentages of iron oxides and CaO in the parent glass.

The sintering was evaluated at 5° and 20°C/min heating rates by measuring the variation of linear shrinkage ($\Delta L/L_0$) referred to the initial 50-mm length. Figure 5 shows the results obtained after 1-h steps at different temperatures. Up to 850°C for G1 and up to

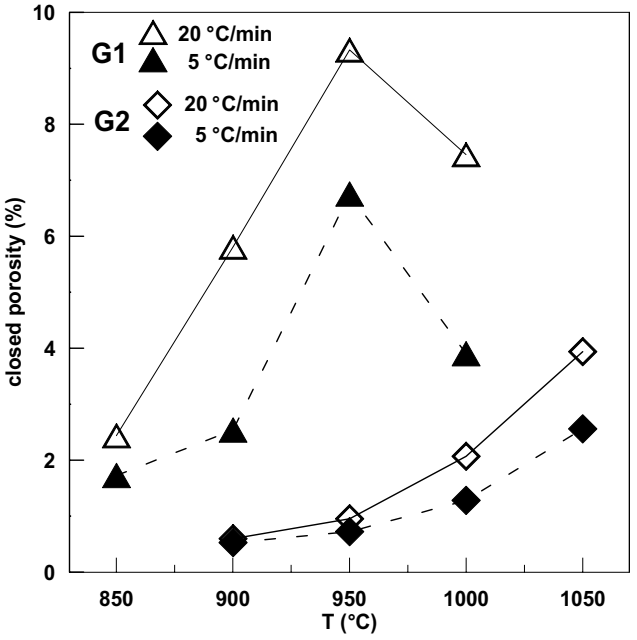

Fig. 7. Percentage of closed porosity after a 1-h step as a function of the holding temperature.

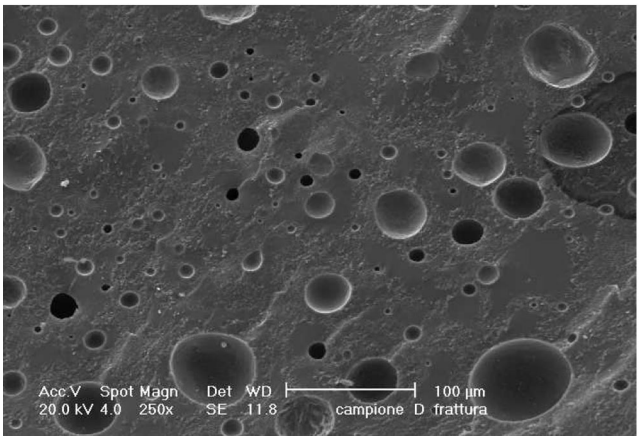

Fig. 8. SEM image of fractured G1 glass-ceramic, heated at 5°C/min and sintered 1 h at 1000°C. (SEM images at 900° and 950°C are available in the Data Depository.)

900°C for G2 (i.e., in the crystallization temperature interval, as observed by DTA) the sintering process is inhibited due to the rapid magnetite precipitation followed by pyroxene crystallization on the magnetite nuclei.[2,7] Then, as shown in the figure, the densification increases as a function of temperature with different behavior for G1 and G2 compositions.

The linear shrinkage of G1 is favored by the low heating rate and increases up to 950°–970°C. Then, at 1000°C, deformation of the samples takes place. In G2, the sintering is favored by the high heating rate, no deformation is observed, and the linear shrinkage reaches higher values.

Figure 6 relates the linear shrinkage as a function of the time at 900°C for G1 and 1000°C for G2. In G1, the initial shrinkage (after 1 min) is 4.5% at 20°C/min and 5.5% at 5°C/min; after about 50 min the maximum value reaches 7.5% at 20°C/min and 8.5% at 5°C/min. G2 shows different behavior: at 5°C/min, the initial shrinkage is 7.5% and increases up to 9.5%, while at 20°C/min the initial value is 9% and the final is 12%.

These differences are due to the different amounts of crystal phase formed in the glass compositions:

(A) G1 forms a relatively low percentage of crystal phase, 25–30 wt%. As a result, at 1000°C the apparent viscosity is low and deformation of the samples occurs. The rate of crystallization, in the low-temperature interval, is relatively slow so the sintering is favored by the 5°C/min heating rate.

(B) G2 forms a higher amount of crystal phase, 45–50 wt%, and the samples show higher densification without deformation. Better sintering is obtained at 20°C/min because the increase of the

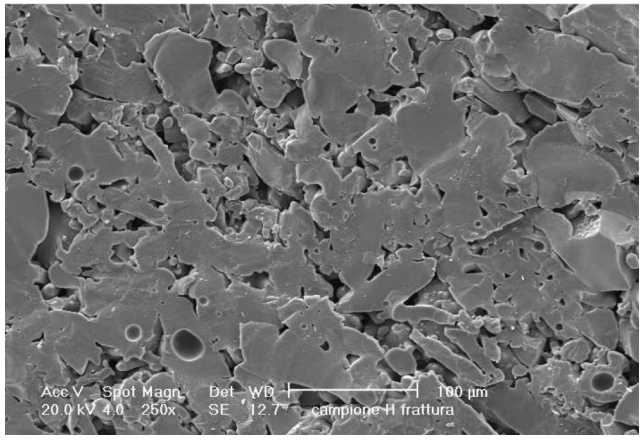

Fig. 9. SEM image of fractured G2 glass-ceramic, heated at 5°C/min and sintered 1 h at 1050°C. (SEM images at 950° and 1000°C are available in the Data Depository.)

Table III. Mechanical Properties of the Obtained Sintered Glass-Ceramics

	Young modulus (GPa)	Bending strength (MPa)	Vickers hardness (MPa)
G1/5	66 ± 2	73 ± 12	4660 ± 100
G1/20	60 ± 4	78 ± 14	3790 ± 40
G2/5	78 ± 4	83 ± 9	6690 ± 20
G2/20	81 ± 4	87 ± 10	6300 ± 20

apparent viscosity (induced by the crystallization) takes place at a higher temperature.

(2) Structure and Properties

The porosity of the sintered samples was evaluated by pycnometry and the morphology observed by SEM.

The percentages of porosity, *P*, were estimated through the following relation:

$$P = 100\,\frac{\rho_u - \rho_a}{\rho_u} \tag{2}$$

where ρ_a and ρ_u are the apparent and ultimate densities of the heat-treated samples obtained before and after milling, respectively.[21] A He displacement pycnometer, which measures the skeleton density of the samples, was used in the present study. Therefore, relation (2) provides the percentage of closed porosity that cannot be filled by the helium. The experimental data are presented in Table II (available in the Data Depository (see footnote ‡ on p. 1)), where the associated error is ± 0003 g/cm^3.

Figure 7 shows the percentages of closed porosity after 1-h heat treatment at different temperatures. In G1, the closed porosity increases with the temperature up to 950°C, reaching 7% at 5°C/min and 8.5% at 20°C/min. At 1000°C, i.e., in the deformation temperature region, the percentage of closed porosity decreases. In G2, the closed porosity is negligible even at 1050°C, so that the structure is mainly characterized by open porosity.

The differences in microstructure were confirmed by SEM observations. Figure 8 shows the fracture morphology of G1 glass-ceramic sintered at 1000°C, while Fig. 9 shows G2 glass-ceramic sintered at 1050°C. (SEM images of G1 glass-ceramics at 900° and 950°C and G2 glass-ceramics at 950° and 1000°C are given in the Data Depository (see footnote ‡ on p. 1).) The differences between G1 and G2 are evident in the closed and open porosity characterizing the two glass-ceramic structures, respectively. At 900°C G1 shows open porosity with necking between the particles; at 950°C the closed porosity is predominant; at 1000°C pore coalescence begins. The sintering of G2 is negligible at 950°C; at 1000°C the formation of the necks starts to take place; at 1050°C the glass-ceramic is sintered, and the structure retains an open porosity.

The mechanical properties, summarized in Table III, were measured using a series of five samples, sintered at 970°C for G1 and at 1050°C for G2. The overall properties of G2 surpass G1 due to the higher amount of crystal phase formed and the lower porosity. The properties, obtained by 5° and 20°C/min heating rates (G1/5, G1/20) and (G2/5, G2/20) are similar for both compositions so that short heat treatment may be applied. Only the G1/5 hardness is higher than G1/20 due to the higher percentage of crystal phase formed. The results show that the obtained values of the bending strength are higher than the characteristic of traditional glazed earthenware ceramics (30–40 MPa), sintered at 1200°–1300°C.[3]

IV. Conclusion

The sintering of iron-rich glass-ceramics is inhibited, in the 750°–900°C crystallization interval, by the intensive magnetite and pyroxene formation; therefore, a higher sintering temperature is required.

In G1 glass-ceramics, a 25%–30% of crystal phase is formed, the densification is favored by low heating rate, and the structure of the material is characterized by closed porosity. In G2, a 45%–50% crystal phase is formed, the sintering is favored by a high heating rate, and the structure shows open porosity.

The obtained glass-ceramics have high mechanical properties which increase as a function of the amount of crystal phase formed. The properties obtained at 5° and 20°C/min heating rates are comparable so that fast heat-treatments may be applied.

Acknowledgments

The authors are grateful to Eng. Giovanni Fedele, Dr. Lorenzo Arrizza, Dr. Monica Ferraris, and Eng. Ildiko Matekovits for the experimental work.

References

[1]B. Locsei, *Molten Silicates and Their Properties*; pp. 44–66. Akademiai Kiado, Budapest, Hungary, 1970.
[2]H. Beall and H. L. Rittler, "Basalt Glass Ceramics," *Am. Ceram. Soc. Bull.*, **55** [6] 579–82 (1976).
[3]J. Hlavac, *The Technology of Glass and Ceramics: An Introduction*; pp. 237–43. Elsevier, Amsterdam, Netherlands, 1983.
[4]L. A Chick, R. O. Lokken, and L. E. Thomas, "Basalt Glass Ceramics for the Immobilization of Transuranicc Nuclear Waste," *Am. Ceram. Soc. Bull.*, **62** [4] 505–10 (1983).
[5]I. W. Donald., B. L. Metcalfe, and R. N. Taylor, "Review—The Immobilization of High Level Radioactive Wastes Using Ceramics and Glasses," *J. Mater. Sci.*, **32**, 5851–87 (1997).
[6]M. Romero and J. Ma. Rincon, "Surface and Bulk Crystallization of Glass-Ceramics in the Na_2O–CaO–ZnO–PbO–Fe_2O_3 System Derived from a Goethite Waste," *J. Am. Ceram. Soc.*, **82** [5] 1313–17 (1999),
[7]A. Karamanov and M. Pelino, "Crystallization Phenomena in Iron Rich Glasses," *J. Non-Cryst. Solids*, **281** [1–3] 139–51 (2001).
[8]M. Pelino, "Recycling of Zinc-Hydrometallurgy Wastes in Glass and Glass-Ceramics Materials," *Waste Manage. (Oxford)*, **20**, 561–68 (2000).
[9]J. Aota, L. Morin, S. Mikhail, T. Chen, and D. Liang, "Immobilization of Hazardous Elements in EAF Dust by Vitrification Process," *Waste Process. Recycl. Miner. Metall. Ind. II, Proc. Int. Symp.*, 335–49 (1995).
[10]A. D. Zunkel, "Electric Arc Furnace Dust Management: A Review of Technologies," *Iron Steel Eng.*, [3] 33–38 (1997).
[11]M. Pelino, A. Karamanov, P. Pisciella, D. Zanneti, and S. Crisucci, "Vitrification of Electric Arc Furnace Dusts," *Waste Manage. (Oxford)*, **22**, 945–49 (2002).
[12]I. Vicente-Mingarro, J. Ma. Rincon, P. Bowles, R. D. Rawlings, and P. S. Rogers, "Viscosity Measurements on Glass Obtained from Alkaline Volkanic Rocks of the Canary Island," *Glass Technol.*, 49–52 (1992).
[13]A. Karamanov, R. Di Gioacchino, P. Pisciella, and M. Pelino, "Viscosity of Iron-Rich Glasses from Industrial Wastes," *Glass Technol.*, **43** [1] 34–38 (2002).
[14]A. Karamanov, G. Taglieri, and M. Pelino, "Iron-Rich Sintered Glass-Ceramics from Industrial Wastes," *J. Am. Ceram. Soc.*, **82** [11] 3012–16 (1999).
[15]J. Ma. Rincon, M. Pelino, and M. Romero, "Glass-Ceramics Obtained from Axial Pressing and Sintering of Vitrified High Iron Content Red Mud"; pp. 169–81 in *Proceedings of the Ist National Congress, "Valorization and Recycling of Industrial Wastes"*. Edited by Mucchi L'Aquila. Modena, Italy, 1997.
[16]J. Ma. Rincon, J. Càcares, C. J. Gonzàlez-Oliver, D. O. Russo, A. Penkova, and H. Hristov, "Thermal and Sintering Behaviour of Basalt Glasses and natural Basalt Powders," *J. Therm. Anal. Calorim.*, **56** 931–38 (1999).
[17]R. Muler, S. Reinish, R. Sojref, and M. Gemeinert, "Sintered Cordierite Glass-Ceramics of Stoichiometric Composition"; *Proceedings of 18th International Congress on Glass* (San Francisco, CA). American Ceramic Socety, Westerville, OH, 1998.
[18]B. Ryu and I. Yasui, "Sintering and Crystallization Behavior of a Glass Powder and Bloks with a Composition of Anorthite and the Microstructure Dependence of Its Thermal Expansion," *J. Mater. Sci.*, **29**, 3323–28 (1994).
[19]Y.-M. Sung, "The Effect of Additives on the Crystallization and Sintering of $2MgO$–$2Al_2O_3$–$5SiO_2$ Glass-Ceramics," *J. Mater. Sci.*, **31**, 5421–27 (1996).
[20]W. Winter, "Sintering and Crystallization of Volume- and Surface-Modified Cordierite Glass Powders," *J. Mater. Sci.*, **32**, 1649–55 (1997).
[21]J. S. Reed., "Density, Pore Structure, and Specific Surface Area"; *Principles of Ceramic Proceedings*, 2nd ed., Ch. 8. Wiley, New York, 1995.
[22]C. S. Ray and D. E. Day, "Nucleation and Crystallization in Glasses As Determined by DTA"; pp. 207–24 in Ceramic Transactions, Vol. 30, *Nucleation and Crystallization in Liquids and Glasses*. Edited by M. C. Weinberg. American Ceramic Society, Westerville, OH, 1992. □